JCB

Supplemental material

van Drogen et al., https://doi.org/10.1083/jcb.201808161

Provided online are two tables in Excel. Table S1 lists confidently assigned phosphorylation sites of Ste5. Table S2 lists confidently assigned phosphorylation sites of Far1.

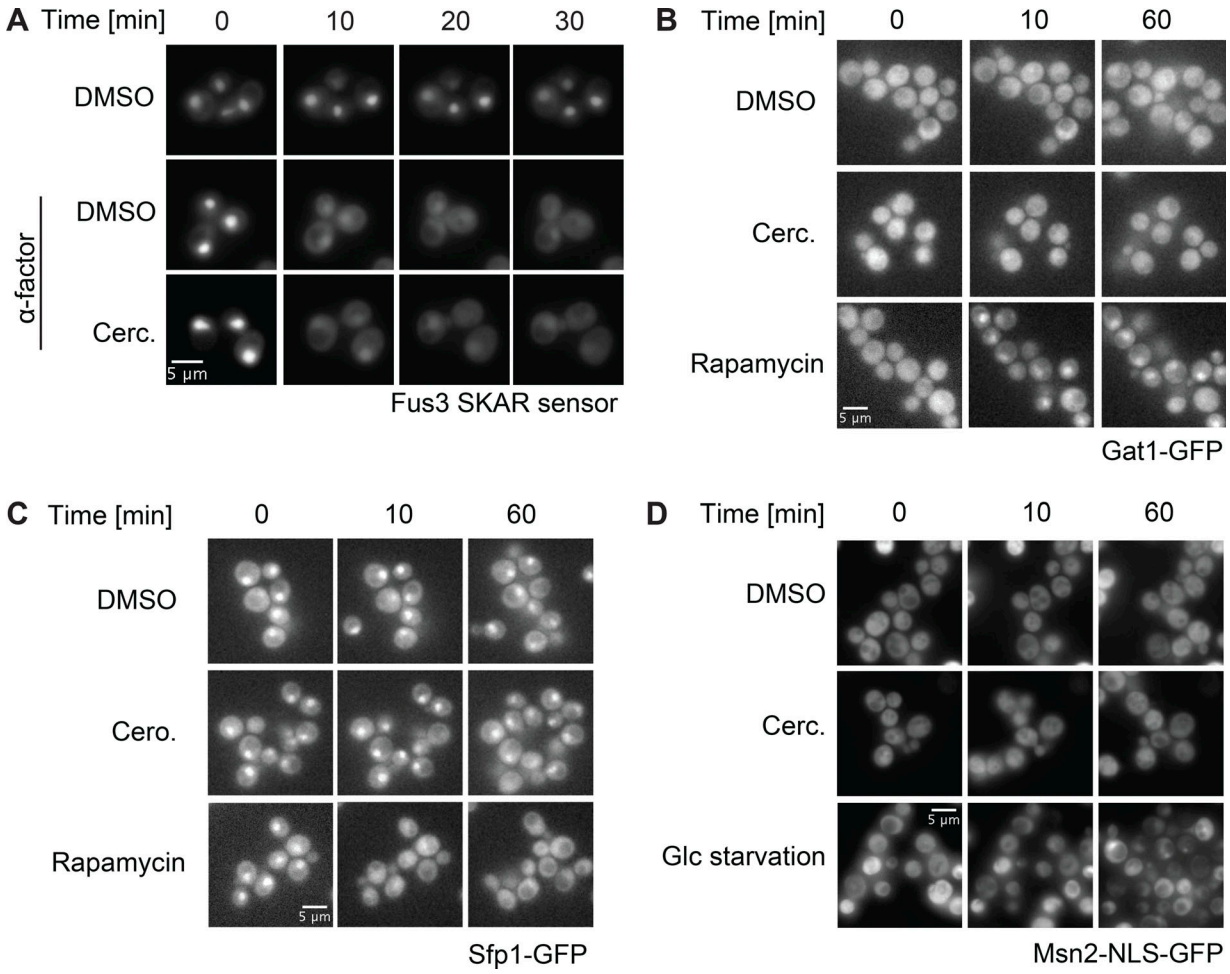

Figure S1. **Specificity of cercosporamide toward Pkc1. (A)** WT cells growing in mid-log phase were loaded in Con A-coated wells. Subsequently, α factor with (cerc.) or without (DMSO) the Pkc1 inhibitor cercosporamide was applied to a final concentration of 7.5 µM (time = 0). Fus3 activity was monitored by fluorescence microscopy using the Fus3 SKARS at the times indicated (minutes). Representative images are shown. Note that the SKAR reporter accumulates in the cytoplasm upon Fus3 activation. **(B)** WT cells expressing Gat1-GFP from the endogenous promoter were exposed at time 0 to DMSO, 7.5 µM cercosporamide (cerc.), or 200 nM rapamycin, and nuclear localization of Gat1-GFP was monitored over time (minutes). Representative images are shown. **(C)** WT cells expressing Sfp1-GFP from the endogenous promoter were exposed at time 0 to DMSO, 7.5 µM cercosporamide (cerc.), or 200 nM rapamycin, and cytoplasmic relocation of Sfp1-GFP was monitored over time (minutes). Representative images are shown. **(D)** WT cells expressing from a 2-µm plasmid a Msn2-NLS-GFP mutant protein that is exclusively regulated by PKA (Görner et al., 2002) were exposed at time 0 to DMSO, 7.5 µM cercosporamide (cerc.), or glucose (Glc) starvation, and nuclear translocation of the Msn2-NLS-GFP reporter was monitored over time (minutes). Representative images are shown. The wells were not coated with Con A (in contrast to A–C).

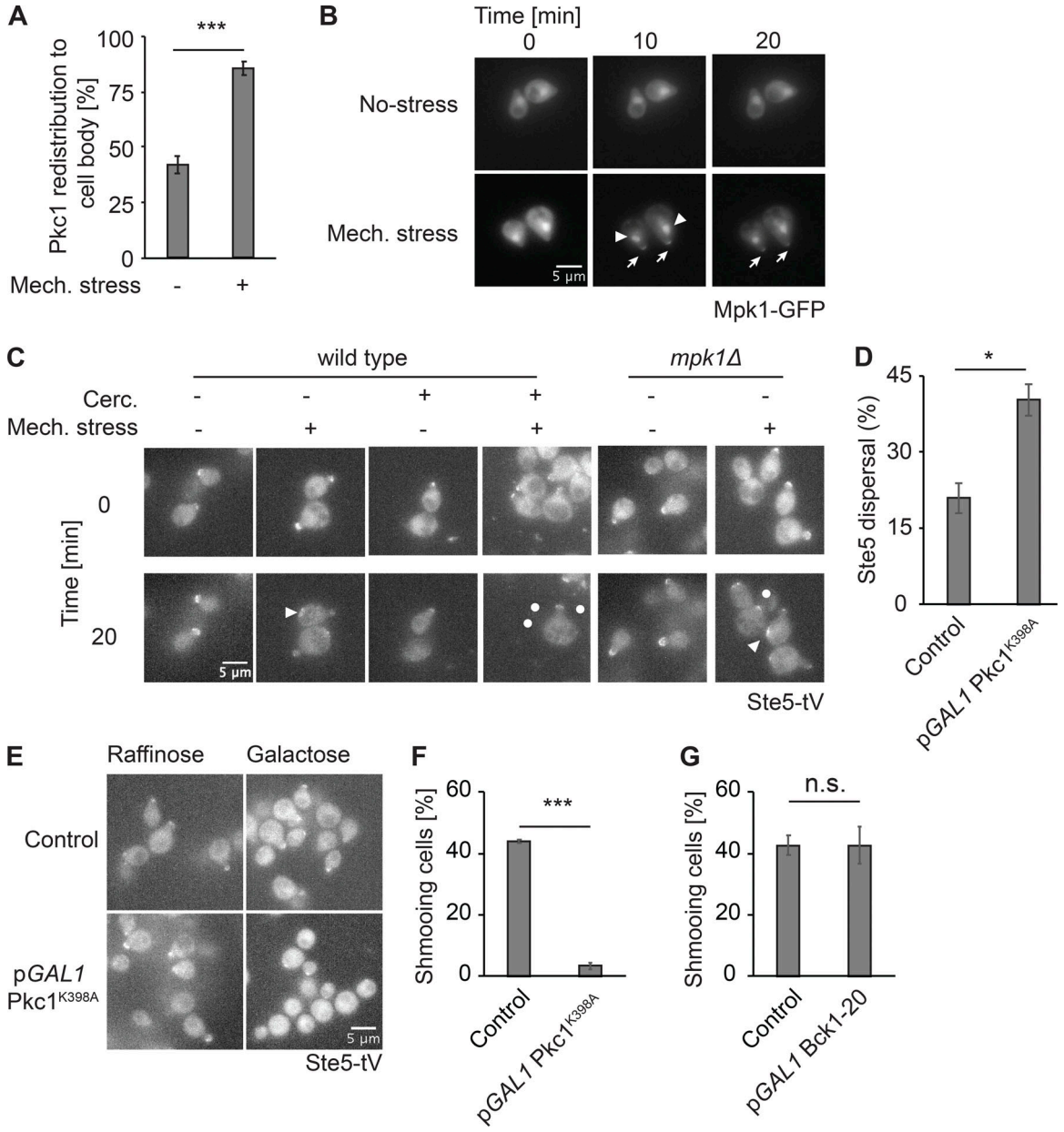

Figure S2. **Pkc1 activation inhibits pheromone response. (A)** Haploid mating-type **a** cells expressing Pkc1-GFP were exposed to 2.7 µM α-factor for 100 min, followed by application of mechanostress (+; 7 psi) or for control no pressure (–) in the microfluidic device. Relocalization of Pkc1-GFP was quantified after 30 min mechanostress for ≥150 cells from three independent experiments. The error bars indicate SEM, and a *t* test was performed to determine statistical significance (***, P ≤ 0.001). **(B)** Haploid mating-type **a** cells expressing Mpk1-GFP were exposed to 2.7 µM α-factor for 100 min, followed by application of mechanostress (+; 7 psi) or, for control, no pressure (–) in the microfluidic device. The nuclear translocation and shmoo tip recruitment of Mpk1-GFP was analyzed microscopically after 30 min of mechanostress. Representative images demonstrating dynamics of Mpk1-GFP during mechanostress to shmoo tips (arrows) and nucleus (arrowheads) are shown. **(C)** Cells expressing Ste5-tV under its endogenous promotor in WT or *mpk1Δ* cells were treated as described in Fig. 1 H, and the localization of Ste5-tV was visualized microscopically in microfluidic chips during 30 min of mechanostress. Representative images are shown. Lysing cells are highlighted with a white dot. Note that in some cases Ste5-tV transiently accumulates at other cortical regions, as indicated by the arrowheads. **(D)** WT cells expressing Ste5-tV under its endogenous promotor were transformed with a plasmid expressing a constitutively active allele of PKC1 (pGAL-Pkc1^{R398A}) from the inducible GAL1 promoter. Cells growing in 2% raffinose were treated with pheromone for 100 min followed by induction of Pkc1^{R398A} with 2% galactose. Loss of Ste5-tV from shmoo tips was visualized microscopically every 10 min in 2 h of induction. Ste5-tV dispersal from shmoo tips was quantified by counting ≥150 cells from three independent experiments. The error bars indicate SEM, and a *t* test was performed to determine statistical significance (*, P ≤ 0.05). **(E)** Cells harboring a galactose inducible Pkc1^{R398A} plasmid (pGAL1-Pkc1^{R398A}) or not (control) were grown to log phase in 2% raffinose. The cells were then shifted to 2% galactose media for 3 h followed by pheromone treatment for 100 min. The shmooing and Ste5 recruitment to shmoo tips was visualized under microscope. Representative images are shown. **(F and G)** Cells expressing galactose inducible Pkc1^{R398A} (F) or Bck1-20 (G) were treated with 2% galactose and subsequently with pheromone for 100 min. The percentage of cells that have formed mating projections (shmoos) among ≥150 cells upon pheromone treatment was quantified from three independent experiments. Error bars indicate SEM, and a *t* test was used to determine statistical significance (NS, P > 0.05; ***, P ≤ 0.001).

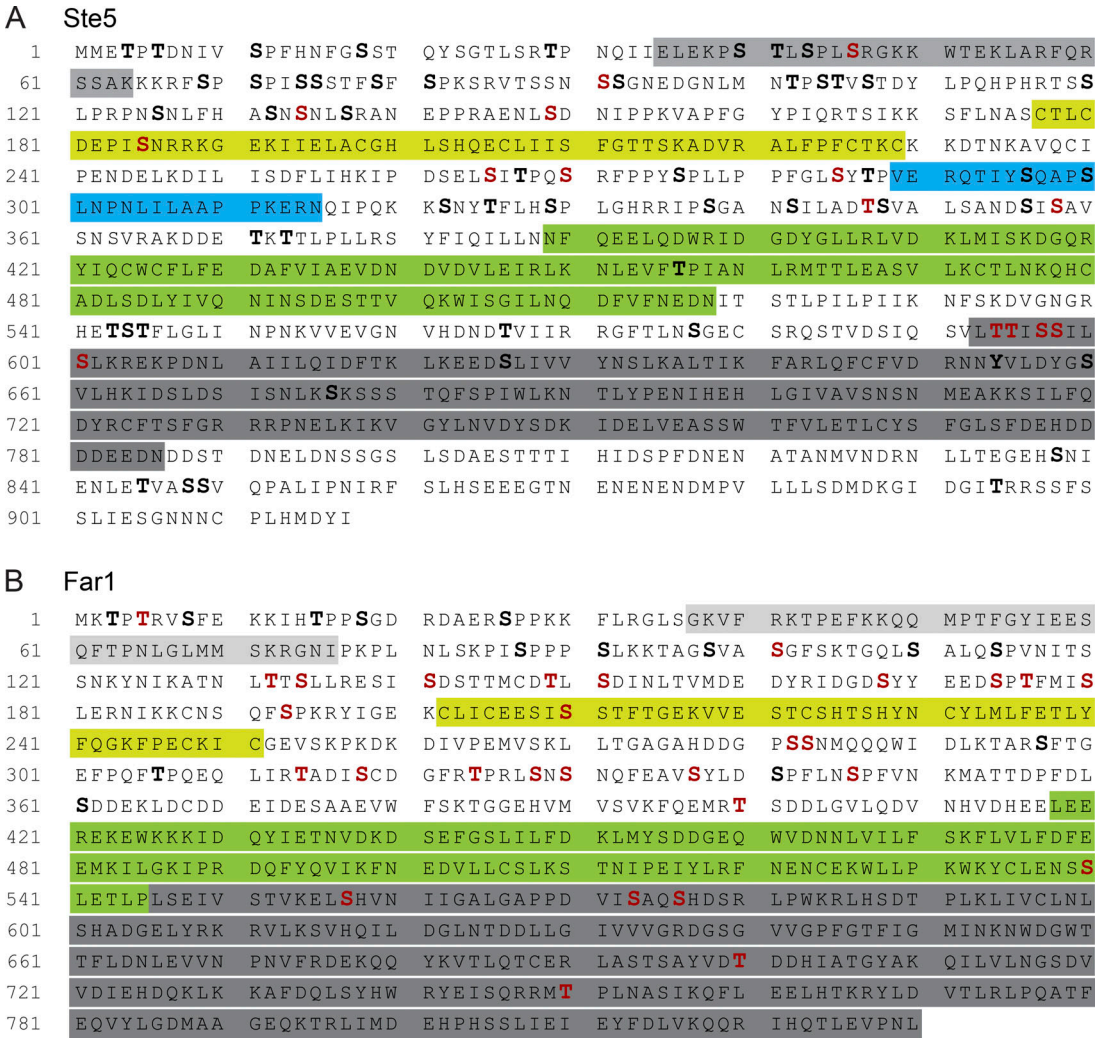

Figure S3. **Mapping of phosphosites on Ste5 and Far1. (A)** The amino acid sequence of *S. cerevisiae* Ste5 with the functional domains color coded as schematically indicated in Fig. 2 A, following the domain boundaries published previously (Good et al., 2009). Gray, PM domain; yellow, RING; light blue, MAPK-docking site; green, PH domain; and dark gray, von Willebrand factor type A domain (VWA). The sites identified by MS analysis as phosphorylated in cells exposed to α-factor after phosphopeptide enrichment on a TiO_2 column are highlighted in bold. Phosphosites that have not been detected in other studies are marked in red. The MS data of the different phosphopeptides are listed in Table S1. The raw files are available in the PRIDE repository (http://www.proteomexchange.org) via the PRIDE partner repository with the dataset identifier PXD004657. **(B)** The amino acid sequence of *S. cerevisiae* Far1 with the functional domains color coded as follows: gray, PM motif; yellow, RING; light blue, Cdc24-binding site; green, PH domain. The sites identified by MS analysis as phosphorylated in cells exposed to α-factor after phosphopeptide enrichment on a TiO_2 column are highlighted in bold. Phosphosites that have not been detected in other studies are marked in red. The MS data of the different phosphopeptides are listed in Table S2. The raw files are available in the PRIDE repository (see above).

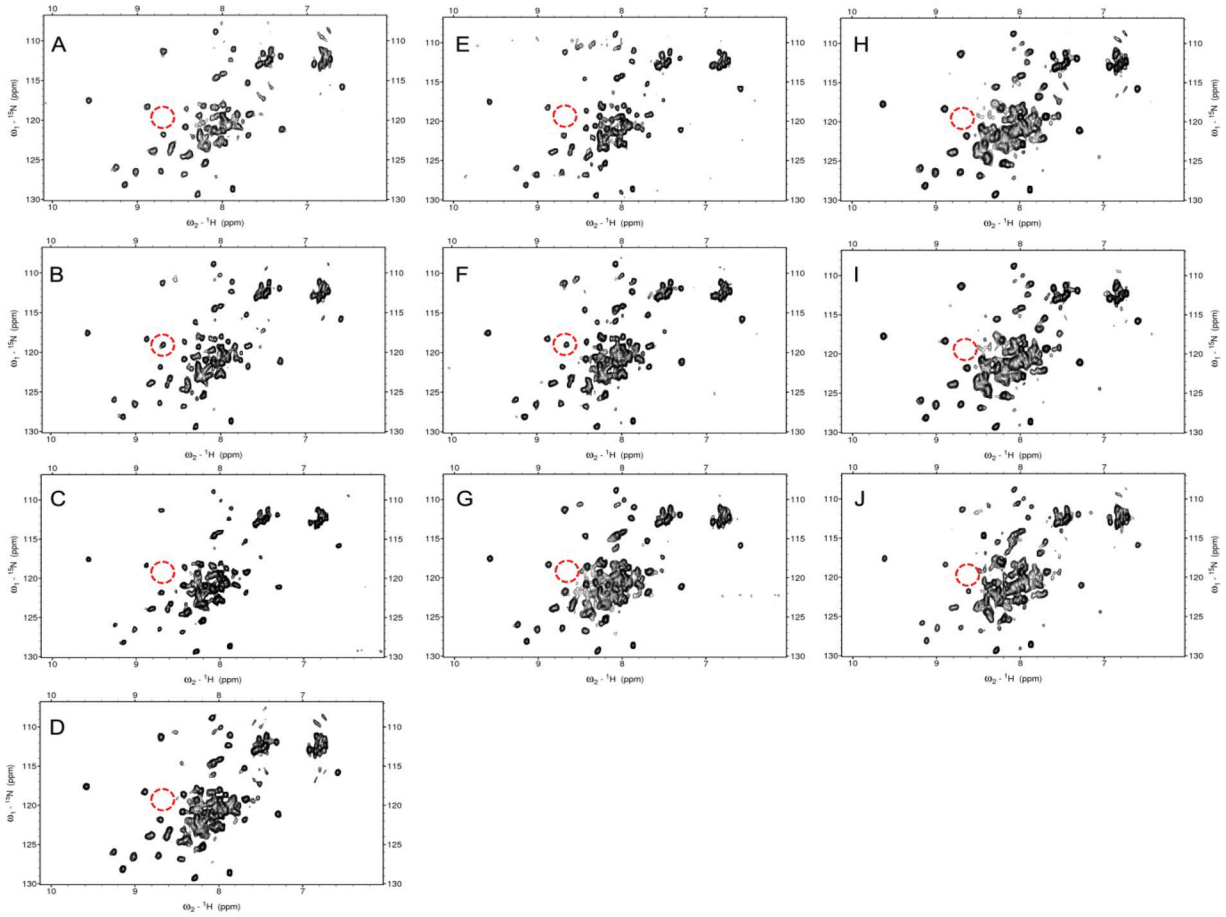

	Ste5 149-238							Ste5 149-238 S185A		
	NB				YE			NB	NB	YE
	A	B	C	D	E	F	G	H	I	J
PKC	-	+	+	+	-	-	-	-	+	-
ATP	-	+	+	+	-	+	+	-	+	+
Inhibitor	-	-	-	+	-	-	+	-	+	-
Activator	-	+	-	+	-	+	+	-	+	+

Figure S4. **NMR-based in vitro phosphorylation assays. (A–J)** In vitro kinase assays analyzed by 600 MHz ^{1}H-^{15}N correlation NMR spectroscopy (SOFAST HMQC; Schanda et al., 2005) using either WT or the nonphosphorylatable S185A mutant RING domain as a substrate and incubated as indicated in the table below with yeast extract (YE; protein concentration of 70 µM) or with or without purified PKCα and in the absence or presence of the inhibitor cercosporamide in NMR buffer (NB). Red dashed circles indicate the resonance position of the amide group of phosphorylated Ser^{185}.

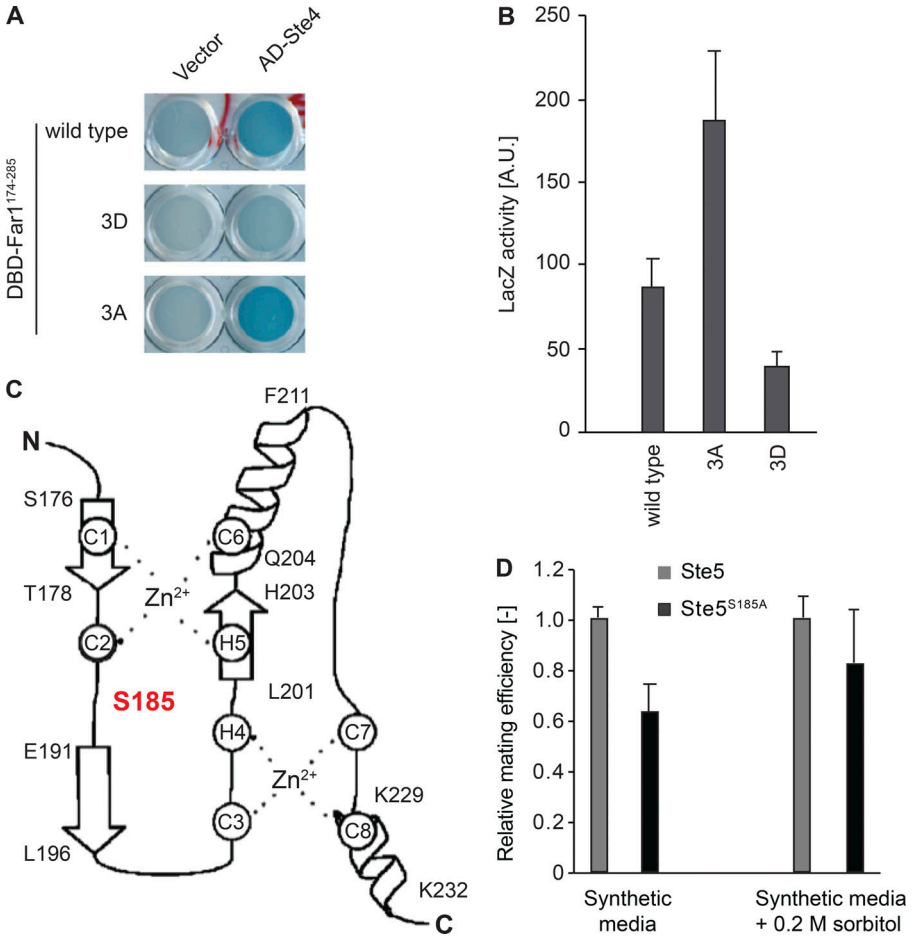

Figure S5. **Two-hybrid analysis of the Far1-RING-H2 domain with Ste4, ste5^{S185A} mating efficiency, and schematic representation of the Ste5 RING-H2 domain structure bound to Gβγ. (A and B)** Yeast two-hybrid analysis of an empty control plasmid (vector) or Ste4 fused to the activation domain (AD) with WT or the indicated nonphosphorylatable (3A) or phospho-mimicking (3D) mutants of the RING-H2 fragment of Far1 (amino acids 174–285), expressed as a fusion to the LexA-DNA–binding domain (DBD). The expression of β-galactosidase was imaged (A) and quantified as described in Materials and methods. Background absorbance measured in the vector control was subtracted and the data plotted as arbitrary units with SDs from three independent experiments. **(C)** The schematic representation of the RING-H2 domain structure bound to Gβγ was deduced from assigning specific residues to sufficiently resolved peaks (approximately 80%) in the [^{1}H, ^{15}N] correlation spectra (Walczak et al., 2014). Secondary structures such as β-sheets and α-helices are indicated, with the amino acids flanking these structural elements. The position of S185 (red) as well as the six cysteines (C) and two histidine (H) residues coordinating the Zn^{2+} ions (dashed lines) are highlighted. The N-terminus and C-terminus of the RING-H2 domain are shown. Note that in complex with the Gβγ heterodimer, the RING-H2 domain seems to adopt a fold characteristic for E3-ubiquitin ligases. Adapted from Walczak et al. (2014). **(D)** The relative mating efficiency of ste5Δ cells expressing either WT Ste5 (gray bars) or Ste5^{S185A} (black bars) was measured in synthetic media or synthetic media containing 0.2 M sorbitol. The SD was determined from at least three experiments. Fig. S5 is reprinted with permission from *Angewandte Chemie International Edition*.

References

Good, M., G. Tang, J. Singleton, A. Reményi, and W.A. Lim. 2009. The Ste5 scaffold directs mating signaling by catalytically unlocking the Fus3 MAP kinase for activation. *Cell.* 136:1085–1097. https://doi.org/10.1016/j.cell.2009.01.049

Görner, W., E. Durchschlag, J. Wolf, E.L. Brown, G. Ammerer, H. Ruis, and C. Schüller. 2002. Acute glucose starvation activates the nuclear localization signal of a stress-specific yeast transcription factor. *EMBO J.* 21:135–144. https://doi.org/10.1093/emboj/21.1.135

Schanda, P., E. Kupče, and B. Brutscher. 2005. SOFAST-HMQC experiments for recording two-dimensional heteronuclear correlation spectra of proteins within a few seconds. *J. Biomol. NMR.* 33:199–211. https://doi.org/10.1007/s10858-005-4425-x

Walczak, M.J., B. Samatanga, F. van Drogen, M. Peter, I. Jelesarov, and G. Wider. 2014. The RING domain of the scaffold protein Ste5 adopts a molten globular character with high thermal and chemical stability. *Angew. Chem. Int. Ed. Engl.* 53:1320–1323. https://doi.org/10.1002/anie.201306702